Respective roles of the glutamine synthetase/glutamate syntase cycle and glutamate dehydrogenase in ammonium and amino acid metabolism during germination and post-germinative growt...

ARTICLE *in* PLANTA · JULY 2004

Impact Factor: 3.26 · DOI: 10.1007/s00425-004-1214-9 · Source: PubMed

Planta (2004) 219: 286–297
DOI 10.1007/s00425-004-1214-9

ORIGINAL ARTICLE

Gaëlle Glevarec · Sophie Bouton · Emmanuel Jaspard
Marie-Thérèse Riou · Jean-Bernard Cliquet
Akira Suzuki · Anis M. Limami

Respective roles of the glutamine synthetase/glutamate synthase cycle and glutamate dehydrogenase in ammonium and amino acid metabolism during germination and post-germinative growth in the model legume *Medicago truncatula*

Received: 8 July 2003 / Accepted: 10 January 2004 / Published online: 26 February 2004

Abstract Our objective was to determine the respective roles of the couple glutamine synthetase/glutamate synthase (GS/GOGAT) and glutamate dehydrogenase (GDH) in ammonium and amino acid metabolism during germination and post-germinative growth in the model legume *Medicago truncatula* Gaertn. For this aim, amino acids were analyzed by HPLC and changes in gene expression of several enzymes involved in N and C metabolism were studied by real-time quantitative reverse transcription–polymerase chain reaction. Among the enzymes studied, GDH showed the highest increase in gene expression (80-fold), specifically in the embryo axis and concomitant with the increase in ammonium content during post-germinative growth. In cotyledons, GDH gene expression was very low. Although in vitro GDH aminating activity was several times higher than its deaminating activity, in vivo $^{15}NH_4$ incorporation into amino acids was completely inhibited by methionine sulfoximine, a GS inhibitor, indicating that GDH is not involved in ammonium assimilation/detoxification. Changes in the expressions of GS and GOGAT isoforms revealed that GS1b (EC 6.3.1.2) in concert with NADH-dependent GOGAT (EC 1.4.1.14) constitute the major route of assimilation of ammonium derived from reserve mobilization and glutamic acid/glutamine synthesis in germinating *M. truncatula* seeds. However, during post-germinative growth, although germination was held in darkness, expression of *GS2* and *Fd-GOGAT* (EC 1.4.7.1) increased and expression of *GS1b* decreased in cotyledons but not in the embryo axis. 2-Oxoglutarate, the substrate of the transamination reaction, was provided by the cytosolic isoform of isocitrate dehydrogenase (EC 1.1.1.42). We suggest that GDH during post-germinative growth, specifically in the developing embryo axis, contributes to ammonium delivery to GS for glutamine synthesis in the absence of primary NO_3^- assimilation. Interestingly, this reaction also produces reducing power (NADH) in organs deprived of photosynthesis.

Keywords Amino acid metabolism · Germination · Glutamate dehydrogenase · Glutamine synthetase/glutamate synthase · *Medicago* · Post-germinative growth

Abbreviations EST: Expressed sequence tag · Fd-GOGAT: Ferredoxin-dependent glutamate synthase · GDH: Glutamate dehydrogenase · GS: Glutamine synthetase · GS1a, GS1b: Cytosolic GS · GS2: Chloroplastic GS · cICDH: Cytosolic isocitrate dehydrogenase · mIDH: Mitochondrial isocitrate dehydrogenase · MSC27: *Medicago sativa* cDNA 27 · MSX: Methionine sulfoximine · NADH-GOGAT: NADH-dependent glutamate synthase · PEPc: Phosphoenolpyruvate carboxylase

G. Glevarec · S. Bouton · E. Jaspard · M.-T. Riou
A. M. Limami (✉)
UMR INRA 1191, Physiologie Moléculaire des semences, University of Angers, 2 Bd Lavoisier, 49045 Angers cedex 01, France
E-mail: anis.limami@univ-angers.fr
Fax: +33-2-41735352

J.-B. Cliquet
UMR INRA 950, Physiologie et Biochimie Végétales, University of Caen, 14032 Caen cedex, France

A. Suzuki
Unité de recherche Nutrition Azotée des Plantes, INRA, Route de St Cyr, 78026 Versailles cedex 01, France

Introduction

Mobilization of reserves has been described as a crucial process that controls germination (Eastmond et al. 2000; Finkelstein and Lynch 2000; Eastmond and Graham 2001; Pritchard et al. 2002). Indeed, germinating seeds deprived of an efficient mineral-uptake system and

photosynthetic apparatus rely on reserve mobilization for germination and development, leading to a nitrogen- and carbon-autotrophic seedling (Bewley 1997; Baskin and Baskin 1998; Koorneef et al. 2002). In particular, mobilization of nitrogen reserves as a source of energy and nutrients to supply expanding new tissue is proposed to take part in the control of germination (Garciarubio et al. 1997). Several analytical works based on ^{14}C labeling showed that amino acids in germinating seeds contribute a large amount of carbon substrate to the respiratory system and sugar synthesis, as shown in gluconeogenic oilseeds such as castor bean (Lea and Joy 1983). Considerable inter-conversion of amino acids occurs following storage-protein hydrolysis in germinating seeds (Lea and Joy 1983). This process contributes to produce a complete spectrum of amino acids that can be used either as protein building blocks or precursors for key metabolites, and that can play determinant roles in control of germination and seedling development (Gallardo et al. 2002).

Glutamate (Glu) is likely to play a pivotal role in inter-conversion of amino acids in germinating seeds. Aminotransferases in plants preferentially use Glu and the corresponding keto-acid 2-oxoglutarate in transamination reactions. Furthermore, Glu is either the precursor or by-product of the degradation of specific amino acids such as Arg, Pro and His (Morot-Gaudry et al. 2001). Glutamate also leads to ammonium release in an oxidative deamination reaction catalyzed by glutamate dehydrogenase (GDH, EC 1.4.1.2; Miflin and Habash 2002). In seeds germinating in darkness, the absence of primary nitrogen (NO_3^-) assimilation and the position of Glu at the centre of amino acid breakdown make this reaction one of the major sources of ammonium for glutamine synthetase (GS, EC 6.3.1.2; Miflin and Habash 2002). In several species, GS isoforms specific to seed tissue or specifically expressed during germination have been isolated (Swarup et al. 1990; Watanabe et al. 1994; Limami et al. 2002).

Since the discovery of glutamate synthase (GOGAT; Lea and Miflin 1974), strong evidence has been produced in favor of the GS/GOGAT cycle rather than GDH as the major pathway of ammonium assimilation in plants (Miflin and Lea 1980; Trepp et al. 1999a, 1999b). However, despite evidence in favor of a catabolic function of GDH in Glu metabolism (Robinson et al. 1991, 1992; Stewart et al. 1995; Aubert et al. 2001), several authors still propose that this enzyme may play an alternative role to the GS/GOGAT cycle in ammonium assimilation under specific physiological conditions that make the ammonium concentration increase. It has been shown that expression of *GDH1-1* in *Arabidopsis thaliana* seedlings is boosted by the addition of ammonium to the growth medium (Melo-Oliveira et al. 1996). While seedlings of the *Arabidopsis* knock-out mutant *gdh1-1* showed the same germination and growth rate as the wild type on organic medium, they displayed a dramatic developmental defect in the presence of ammonium. These observations suggest that GDH may play an accessory role in primary nitrogen assimilation (Melo-Oliveira et al. 1996). It was also proposed that GDH would assimilate ammonium in tobacco source leaves during senescence to compensate for the decrease in ferredoxin-dependent GOGAT (Fd-GOGAT; Masclaux-Daubresse et al. 2002). Nonetheless, except for the synthesis of [^{15}N]Glu from $^{15}NH_4$ by isolated pea and corn root mitochondria (Yamaya et al. 1986), evidence to support the alternative role of GDH is to our knowledge entirely based on in vitro changes in aminating/deaminating GDH activity associated with changes in gene expression. Furthermore, this evidence is weakened by the fact that in vitro GDH activity tests are not reliable in validating a metabolic role (Fricke and Pahlich 1992).

Germination sensu stricto starts with imbibition and ends up with radicle emergence followed by a period of development called post-germinative growth that ends up with the acquisition of autotrophy. During these two periods, seedlings are heterotrophic in the sense that they completely depend on seed reserves. The objective of our work was to characterize amino acid metabolism, N and C interactions during germination and post-germinative growth, in darkness and in the absence of NO_3^-, with a particular focus on the role of GDH in Glu and ammonium metabolism. We carried out this work on the model legume *Medicago truncatula* for two reasons. First, the major reserves in legume seeds are nitrogenous compounds and, second, few studies have been done on reserve mobilization and metabolism in germinating legume seeds compared to oilseeds (*Arabidopsis thaliana*) and starch-accumulating seeds (rice and barley). By using 2-oxoglutarate delivered by the cytosolic isocitrate dehydrogenase (cICDH, EC 1.1.1.42), we have shown that, in germinating seed, ammonium is assimilated by the cytosolic GS1b in concert with NADH-dependent GOGAT (NADH-GOGAT). Concomitant with the increase in ammonium content, both GDH gene expression and protein increased in the embryo axis but not in cotyledons. Although in vitro aminating GDH activity was several times higher than deaminating activity, in vivo $^{15}NH_4$ incorporation into amino acids was completely inhibited by the GS inhibitor methionine sulfoximine (MSX), indicating that GDH is not involved in ammonium assimilation/detoxification. We suggest that in germinating seeds, in the absence of nitrogen (NO_3^-) primary assimilation, GDH is rather involved in Glu catabolism, which generates ammonium, the substrate for glutamine (Gln) synthesis by GS, and reducing power (NADH).

Materials and methods

Seeds and germination conditions

Seeds of *Medicago truncatula* Gaertn. (cv. Paraggio) were germinated in petri dishes (diameter 9 cm) on Whatman paper soaked with 3.5 ml de-ionized water, and maintained in a growth chamber in darkness at 20°C. Three replicates of 50 grains per petri dish

were used for the germination test, i.e. determination of T50, the time at which 50% of seeds germinated. Germination corresponded to emergence of the radicle.

For further biochemical analysis, germinated seeds were sampled at various times throughout the germination process from 0 to 48 h. For all samples, the seed coat and albumen were removed. Cotyledons and the embryo axis were collected separately and frozen in liquid nitrogen before being stored at −80°C.

Extraction and analysis of metabolites

Frozen plant material was used for metabolite extraction. Samples were agitated for 1 h in 96% ethanol at 4°C. After centrifugation the ethanol fraction was removed and the same process was then repeated with water. The ethanol and water fractions were combined and stored at −20°C (Vincent et al. 1997) for further analysis. Neutral sugars glucose, fructose and sucrose and organic acids citrate, malate and oxaloacetate were measured enzymatically using commercial kits (Roche, Mannheim, Germany). 2-Oxoglutarate was extracted with 1 M $HClO_4$ as described by Ferrario-Méry et al. (2002) and measured enzymatically according to Bergmeyer (1965). Free NH_4^+ was determined by the phenol hypochlorite assay (Berthelot reaction). Individual amino acids were determined by HPLC by derivatization with phenylisothiocyanate (PITC) (Fluka, Hanover, Germany). PITC reacts with primary and secondary amines, leading to phenylthiocarbamyl (PTC)-amino acids detectable at 254 nm. Total amino acids (8 mmol) and standard amino acids plus homoserine (30–100 μmol) were first neutralized with 1 ml ethanol:water:triethylamine (2:2:1, by vol.) and vacuum-dried. Samples were then derivatized by the addition of 500 μl ethanol:water:triethylamine:PITC (7:1:1:1, by vol.) corresponding to 5 times PITC excess (mol/mol). Samples were incubated for 30 min at room temperature and vacuum-dried. PTC-amino acids were dissolved in ethanol:water (1:1 for plant amino acids and at various ratios depending on the hydrophobic nature of the PTC-amino acid for the standards) and stored at −20°C before HPLC analysis. Reverse-phase HPLC was performed using a Waters system (Millipore) with two 510 pumps, a 484 absorbance detector and an injection valve model 7725i (Rheodyne). System control and data processing were performed using Millennium 32 chromatography manager software (Waters). Derivatized amino acids were loaded on a Waters Nova-Pak 4 μm C_{18} column (300 mm long, 3.9 mm i.d.) thermostatted at 37°C and operated at a flow rate of 1.0 ml min^{-1}. PTC-amino acids were separated and eluted using two mobile phases (solvent A: 20 mM aqueous sodium acetate, 0.04% trifluoroacetic acid and 0.04% triethylamine; solvent B: acetonitrile) and a discontinuous gradient as follows: 7–9% B over 10 min, 9–22% B over 3 min, 22–32% B over 10 min, 32–80% B over 3 min, 80–7% B over 3 min and re-equilibration at 7% for 3 min.

Enzyme assays

Glutamine synthetase and glutamate dehydrogenase Enzymes were extracted from 25 mg of frozen plant material in 1.5 ml of Tris–HCl buffer (25 mM, pH 7.6) supplemented with 1 mM $MgCl_2$, 1 mM EDTA, 1 μl ml^{-1} 2-mercaptoethanol and 1% (w/v) polyvinylpolypyrrolidone. The homogenate was centrifuged and the supernatant was used as the crude extract. The protein content was determined colorimetrically using the Bradford method (Bradford 1976).

GS activity was measured on 100 μl of the crude extract in a reaction mixture containing Tris–HCl buffer (50 mM, pH 7,6) supplemented with 20 mM $MgSO_4$, 80 mM Glu, 6 mM hydroxylamine, 4 mM EDTA and 8 mM ATP. The reaction was stopped after 30 min at 30°C by the addition of $FeCl_3$ reagent and centrifuged. γ-Glutamyl hydroxamate (GHM) formed from hydroxylamine and Glu was determined colorimetrically at 540 nm after complexation with $FeCl_3$.

Aminating-GDH activity was assayed by following the oxidation of NADH at 340 nm. Activity was measured on 20 μl of the crude extract in a reaction mixture containing Tris–HCl buffer (100 mM, pH 8) supplemented with 1 mM $CaCl_2$ (pH 8), 13 mM 2-oxoglutarate, 50 mM $(NH_4)_2SO_4$ and 0.25 mM NADH. Deaminating-GDH activity was assayed by following the reduction of NAD. The reaction mixture contained Tris–HCl buffer (100 mM, pH 9) supplemented with 1 mM $CaCl_2$ (pH 9), 33 mM Glu and 0.25 mM NAD or NADP.

Phosphoenolpyruvate carboxylase (PEPc) Enzyme was extracted in Tris–HCl buffer (100 mM, pH 8) supplemented with 20% glycerol, 10 mM $MgCl_2$, 5 mM NaF, 1 μl ml^{-1} 2-mercaptoethanol, 1 mM phenylmethylsulfonyl fluoride (PMSF), 20 μM leupeptin and 2% (w/v) polyvinylpolypyrrolidone. PEPc activity was measured by the coupling of this activity to malate dehydrogenase, which transforms oxaloacetate produced by PEPc into malate, using NADH as reducing power. The assay mixture contained Hepes–KOH buffer (50 mM, pH 8) supplemented with 5 mM $MgCl_2$, 5 mM NaF, 1 mM $NaHCO_3$, 0,2 mM NADH, 3 mM PEP and 10 U ml^{-1} malate dehydrogenase.

$^{15}NH_4$ labeling experiment

Medicago truncatula seeds were germinated in petri dishes as described above on Whatman paper imbibed with water (control) or aqueous 5 mM MSX (Sigma, St-Louis, MO, USA), an inhibitor of GS. After 19 h of imbibition, control seeds and MSX-treated seeds were transferred to petri dishes with the same initial medium to which had been added 2 mM $(^{15}NH4)_2SO_4$ (99% ^{15}N; Euriso-top, Saarbrüken, Germany). Seeds were harvested at the beginning and after 10 h of labeling. They were rinsed twice with distilled water, separated into cotyledons and embryo axis and stored at −80°C. Total amino acids were extracted with ethanol and water as described previously. After evaporation of the extract under vacuum, organic residues were dissolved in distilled water and extracted with the same volume of chloroform. After centrifugation, an aqueous phase containing amino acids was vacuum-dried. Then, amino acids were re-dissolved in distilled water and passed through a 2-ml column of Dowex 50WX8 (200–400 mesh, H-form resin; Supelco, Bellefonte, PA, USA). Columns were washed three times with 1 ml of water, and amino acids were eluted with 5 ml of 6 M NH_4OH. Samples were vacuum-dried and derivatized using N-methyl-N-(tert-butyldimethylsilyl)-trifluoroacetamide (Alltech, Templemars, France) for 30 min at 90°C, as described by Rhodes et al. (1989). Butyldimethylsilyl (BDMS) derivatives obtained were analyzed by GC–MS with a Fisons MD800 quadrupole GC–MS system in order to determine incorporation of ^{15}N into amino acid. A sample of 0.4 μl was injected into the gas chromatograph, which was fitted with an on-column injector, and a fused silica capillary column (30 M methylpolysiloxane, 0.25 μm film thickness). Helium was used as a carrier gas at a flow rate of 1 ml min^{-1}, and the oven was temperature-programmed from 60°C for 1 min, +30°C min^{-1} to 120°C, and from 120°C to 260°C at 8°C min^{-1}. Mass spectra were acquired with an electron energy of 70 eV, and the mass range scanned from mass-to-charge ratios 50 to 650 with a total scan time of 0.9 s. Incorporation of ^{15}N (atom% excess) was calculated after integrating the areas obtained for fragment ions for both labeled and unlabeled amino acids. BDMS derivatives allow the determination of the total amount of ^{15}N incorporated into amino acids and the proportion of amides that are singly and doubly labeled.

Real-time reverse transcription–polymerase chain reaction (RT–PCR)

RNA extraction and reverse transcription Total RNA from embryo axes and cotyledons of seeds imbibed for 10, 15, 21, 25, 37 and 48 h was extracted using TRIzol Reagent (Invitrogen, Breda, The

Netherlands) according to the manufacturer's protocol. A 2-μg sample of total RNA was retrotranscribed for 1 h at 37°C, using 200 units of M-MLV Reverse Transcriptase (Promega, Madison, WI, USA) and 2 μg of $pd(N)_6$ Random Hexamer (Amersham Biosciences, Freiburg, Germany) in the presence of 40 units of Recombinant Rnasin Ribonuclease Inhibitor (Promega), and in a final volume of 50 μl. Genomic DNA was removed by purifying the first strands using a QIAquick PCR Purification Kit (Qiagen, German Town, MD, USA).

Real-time PCR and SYBR Green detection PCR was performed on the light cycler ABI Prism 7000 SDS (Applied Biosystems, Foster city, CA, USA) with the SYBR Green PCR Master Mix (Applied Biosystems) according to the manufacturer's protocol. Each reaction was performed on 5 μl of a 1:2 (v/v) dilution of the first cDNA strands, synthesized as described above with 0.3 μM of each primer in a total reaction of 20 μl. The reactions were incubated for 2 min at 50°C and 10 min at 95°C followed by 60 cycles of 15 s at 95°C and 1 min at 60°C. The specificity of the PCR amplification procedures was checked with a heat-dissociation protocol (from 65°C to 95°C) after the final cycle of the PCR. Each reaction was done in triplicate and the corresponding Ct values were determined.

Amplified fragments of each gene were cloned into pGEM-T Easy vector (Promega). The plasmids were diluted several times to generate templates ranging from 10^5 to 10^3 copies used for standard curves for the estimation of copy numbers. The results are expressed as copy number of cDNA corresponding to each gene studied in 5 μl of first strands.

Expressed sequence tags (ESTs) from the Toulouse *Medicago truncatula* database (http://medicago.toulouse. inra.fr/ Mt/ EST/) were used to design primer sets for the amplification of each gene (Table 1).

Results

Germination and changes in nitrogen and carbon metabolites and organic acids

Medicago truncatula seeds were germinated in darkness at 20°C in the absence of NO_3^-. The dynamic of germination and water uptake fitted within the classical three-step model described by Bewley (1997). The first step characterized by fast water uptake (0–6 h) was followed by a second step characterized by a slowdown in water uptake, an increase in metabolic activity and radicle protrusion, which occurred 23 h after the beginning of imbibition in the present experiment. The two first steps correspond to germination sensu stricto (Bewley 1997). The third step corresponds to post-germinative growth, characterized by an increase in water uptake and ending with seedling establishment and acquisition of autotrophy (Bewley 1997). During both germination sensu stricto and post-germinative growth, seedlings are heterotrophic, relying only on seed reserves. They are submitted essentially to molecular-physiological changes that allow for reserve mobilization and utilization before the acquisition of autotrophy. At the morphological level, only a few changes are observed, corresponding to radicle protrusion at the end of germination sensu stricto and an increase in root length up to 2 cm during post-germinative growth, while cotyledons remain white and turgescent. The increase in biomass in the absence of light and nutrient supply (nitrate) corresponds only to an increase in fresh weight due to water uptake.

Nitrogen metabolites (ammonium and total amino acids), soluble sugars (sucrose, glucose and fructose) and organic acids (citrate, malate, 2-oxoglutarate and oxaloacetate) were measured in the dry seed (0 h) and from 5 to 48 h of imbibition in embryo axis and cotyledons separately.

The total amount of free amino acids in the dry seed was 1,413 nmol, represented essentially (62%) by Arg, Tyr and Asn (Fig. 1). Throughout germination the amino acid pool showed both quantitative and qualitative changes. The total amount of amino acids slightly increased during the first hours of imbibition. At 21 h, immediately before radicle emergence, cotyledons and embryo axis contained 1,864 and 665 nmol, respectively, which represented a 1.7-fold increase in total seed amino acids compared to the dry seed. After radicle emergence, the total amount of amino acids sharply increased; at 48 h, cotyledons and embryo axis contained, respectively, 5,404 and 13,006 nmol, representing a 13-fold increase in total seed amino acids compared to the dry seed (Fig. 1). In contrast to the early stages of germination, the amount of free amino acids in the embryo axis in the late stages of germination was 2.4-fold higher than that in cotyledons. There were also noticeable qualitative differences between the amino acid compositions of cotyledons and embryo axis. Major amino acids in cotyledons were Trp, Asn, His and Arg, representing 65% of total amino acids, whereas in the embryo axis the majority of amino acids (66%) were accounted

Table 1 Primer sets for real-time quantitative PCR amplification. EST sequences from the Toulouse *Medicago truncatula* database (http://medicago.toulouse.inra.fr/Mt/EST/) were used to design primer sets for the amplification of each gene. Primers for specific amplification of *GS1a* and *GS1b* target specific sequences in the 3′ non-translated region

Gene	Forward primer	Reverse primer
MSC27	5′-GTTGAAGTAGACATTGGTGCTAACG	5′-AGCTGAGTCATCAACACCCTCAT
GS1a	5′-GTCCAAGTGGTCTTTAAGCACAAA	5′GAGTAAAATCAAGAAGCAACCATGTTA
GS1b	5′-ACCACCATTCTCTGGAAACCAT	5′-ACAATGCATGTGTGTGTTTTATAGCA
GS2	5′GTTATTGGTTATGAGATGAATGCACAT	5′-TGCAACTCTGTCCATACCATATGC
GDH	5′-GTCCTCTTTGCAACTGAGGCTT	5′-TAATTGTGCAGCCCATGACC
Fd-GOGAT	5′-GCACTGTTGCATCCGGG	5′-TCCTGCATGTTTGATGGAACTT
NADH-GOGAT	5′-CAGGTGACTCTCGGCGTG	5′-TCTTTGGTGAGGTAGCTGTCAACT
ICDH	5′-GTGGAGAAACCAGCACAAACAG	5′-TGGGCTAGACCTCTTTGCCAA
IDH	5′CCCCAAATCTGTATGGAAATCTAGTT	5′-CCTGGCATGACTCCAGTGC

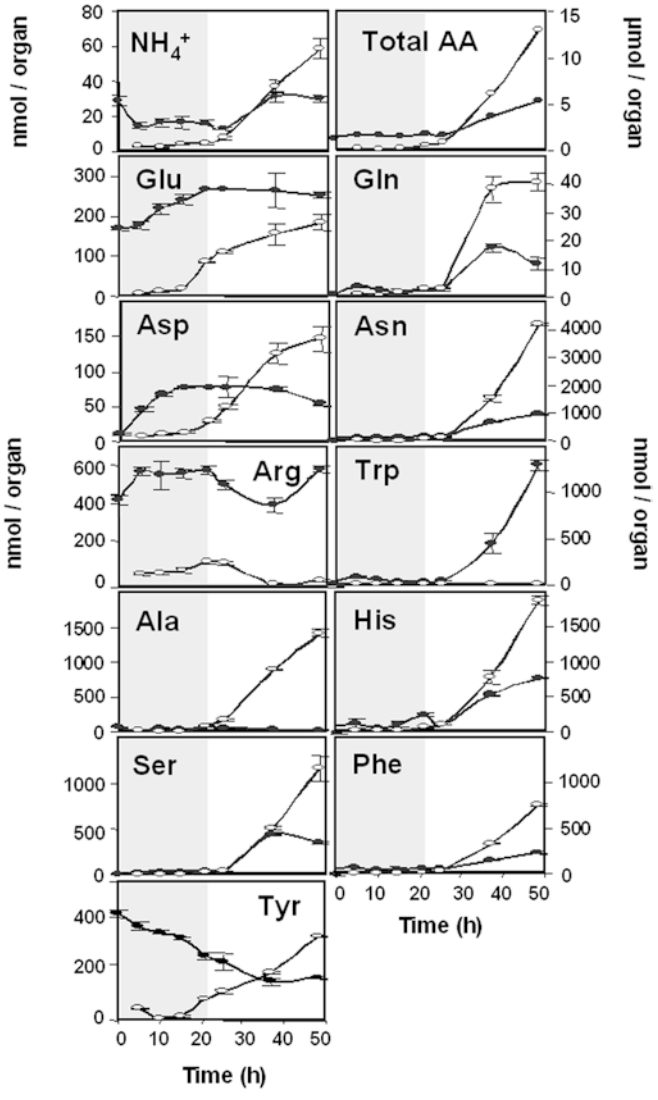

Fig. 1 Changes in amounts of ammonium (NH_4^+), total amino acids (*Total AA*), glutamate (*Glu*), glutamine (*Gln*), aspartate (*Asp*), asparagine (*Asn*), arginine (*Arg*), tryptophan (*Trp*), alanine (*Ala*), histidine (*His*), serine (*Ser*), phenylalanine (*Phe*) and tyrosine (*Tyr*) in cotyledons (*black symbols*) and embryo axis (*white symbols*) throughout germination (*shaded area*) and post-germinative (*non-shaded area*) growth of *Medicago truncatula*. Amounts of all amino acids determined by HPLC were summed up for determination of total amount of amino acids. Results are the mean ± SE of three replicates

for by Asn, His, Ala and Ser. Glutamine did not accumulate appreciably either in cotyledons or in the embryo axis, although its amount increased slightly after radicle protrusion and then stabilized at a low level. At 48 h, the amount of Gln in the embryo axis was 100 times lower than that of Asn. The amount of Glu increased in both cotyledons and embryo axis during the early phases of germination and remained remarkably constant during post-germinative growth (Fig. 1).

The amount of ammonium changed similarly to that of amino acids: it was low and stable in the early stages of germination and increased sharply after radicle emergence, essentially in the embryo axis (Fig. 1).

Amounts of glucose and fructose were very low before radicle emergence (Fig. 2). Afterwards, they remained at a hardly detectable level in cotyledons whereas they increased sharply in the embryo axis. The amount of sucrose increased significantly in the embryo axis throughout germination. In cotyledons, the amount of sucrose increased dramatically in the first hours of imbibition up to 15 h, remained constant during post-germinative growth and dropped at 48 h, probably as result of the exhaustion of carbon (starch) reserves (data not shown).

The amount of citrate in cotyledons decreased in the first hours of imbibition, then remained nearly constant throughout the germination process. In the embryo axis, the amount of citrate increased in the late stages of germination to reach almost the same amount as in cotyledons at 48 h. Oxaloacetate was detected only in cotyledons where its amount remained stable throughout germination. Malate and 2-oxoglutarate were not detected either in cotyledons or in the embryo axis (Fig. 3).

Changes in expression of genes of nitrogen and carbon metabolism enzymes: glutamine synthetase (*GS1a*, *GS1b* and *GS2*), glutamate synthase (*Fd-GOGAT* and *NADH-GOGAT*), glutamate dehydrogenase (GDH), isocitrate dehydrogenase (*cICDH* and *mIDH*)

The expression of genes encoding enzymes involved in N and C metabolism was studied by real-time quantitative RT–PCR in both embryo axis and cotyledons at various times throughout germination. The gene encoding the transcription factor MSC27 (*Medicago sativa* cDNA 27) was used as a constitutive control (Fig. 4i).

There are three GS genes encoding two cytosolic isoforms (*GS1a* and *GS1b*) and one plastidic isoform (*GS2*). The predominant GS gene expressed in germinating seeds was the cytosolic *GS1b*, with an expression 5- to 10-fold higher than that of the cytosolic *GS1a* and the plastidic *GS2* (Fig. 4a–c). In cotyledons, however, during post-germinative growth, from 37 h onwards expression of *GS1b* decreased and that of *GS2* increased concomitantly, whereas the expression of *GS1a* remained very low.

The genes for both NADH-GOGAT and Fd-GOGAT were expressed in germinating seeds. *NADH-GOGAT* was expressed at 10 times the level of *Fd-GOGAT* in the embryo axis throughout germination. In cotyledons, expression of *NADH-GOGAT* was also significantly higher than that of *Fd-GOGAT* up to radicle emergence. A relatively high amount of *Fd-GOGAT* transcripts was found in the early stages of germination in cotyledons; this level decreased thereafter to reach its minimum at 21 h, indicating a decrease in gene transcription. The decrease may also have been due to a low level of transcription during the early stages of germination that did not compensate for the degradation of residual messengers stored in the dry seed. The low and stable level of

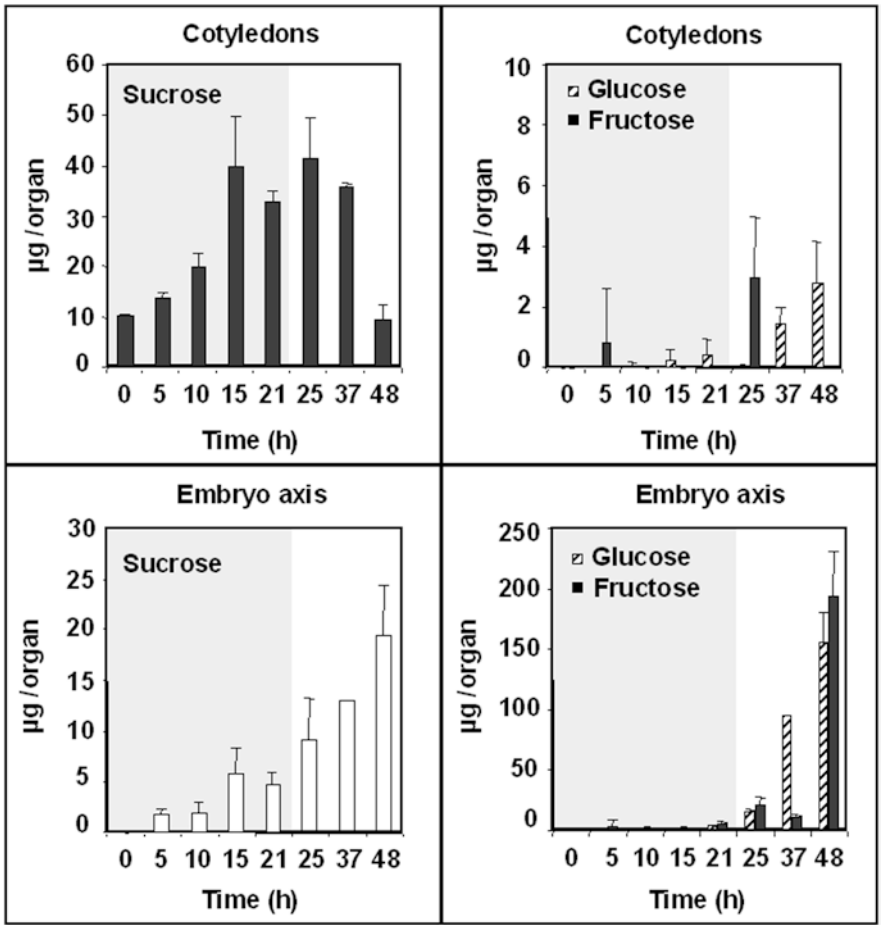

Fig. 2 Changes in amounts of soluble carbohydrates glucose, fructose and sucrose in cotyledons and embryo axis throughout germination and post-germinative growth of *M. truncatula*. *Shaded* and *non-shaded* areas correspond respectively to germination sensu stricto and post-germinative growth. Results are the mean ± SE of three replicates

Fd-GOGAT protein in the seed during the early stages of germination make the second hypothesis more likely. During post-germinative growth, from 37 h onwards, *Fd-GOGAT* expression increased dramatically, becoming almost equal to that of *NADH-GOGAT*. It is interesting to note that this increase in *Fd-GOGAT* expression coincided with the increase in expression of *GS2*.

The gene for GDH was essentially expressed in the embryo axis where its transcripts remained at a relatively low and constant level up to 21 h, before increasing massively (80-fold) during post-germinative growth. Expression in cotyledons was very low, characterized by a decrease during the early stages of germination and an increase during very late stages of germination (48 h).

The expression of genes encoding cytosolic (*cICDH*) and mitochondrial (*mIDH*) isocitrate dehydrogenase was also studied in both embryo axis and cotyledons. Expression of both genes in cotyledons seemed constant throughout the germination period. In contrast, expression of the two genes increased substantially in the embryo axis during post-germinative growth. *cICDH* was, however, the predominant isoform in germinating seeds; its level of expression was 2–4 times higher than that of *mIDH* in the embryo axis or cotyledons (Fig. 4g,h).

Activities of ammonium assimilating and anapleurotic enzymes

Glutamine synthetase activity was measured in the dry seed, cotyledons and embryo axis at various times throughout germination (Fig. 5). Activity was stable and similar in both cotyledons and embryo axis during early phases of germination up to radicle emergence. During post-germinative growth, GS activity did not change significantly in cotyledons but decreased in the embryo axis.

Glutamate dehydrogenase catalyses in vitro a reversible reaction of oxidative NAD-dependent deamination of Glu and reductive NADH-dependent amination of 2-oxoglutarate. The enzyme was active in both directions in vitro; the mean value of aminating activity was at least 3 times higher than that of deaminating activity throughout germination.

Anapleurotic enzymes interfere with nitrogen metabolism by generating carbon skeletons used as substrates by enzymes of amino acids biosynthesis. Activities of both PEPc and isocitrate dehydrogenase were measured in the dry seed as well as in germinating seeds at various times throughout germination (Fig. 6). Their activities showed a similar pattern, decreasing

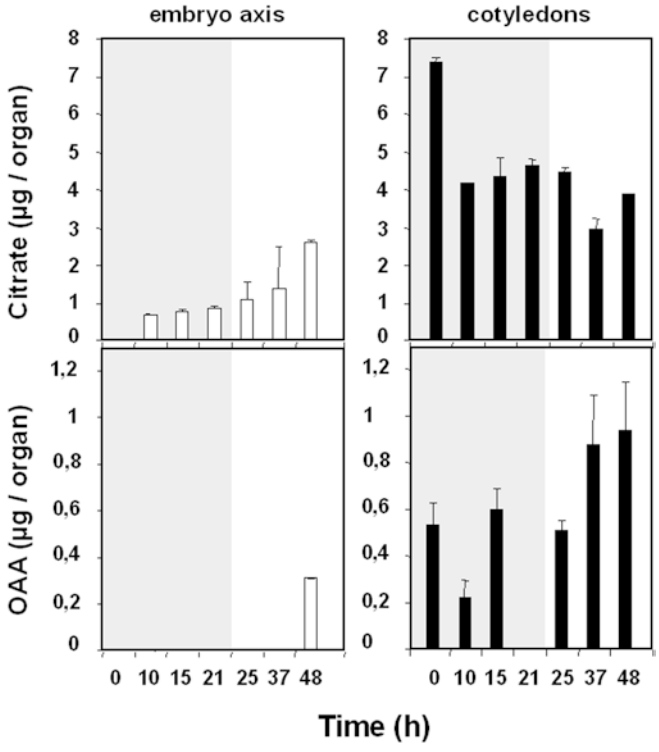

Fig. 3 Changes in amounts of organic acids citrate and oxaloacetate in cotyledons (*black columns*) and embryo axis (*white columns*) throughout germination and post-germinative growth of *Medicago truncatula*. *Shaded* and *non-shaded* areas correspond respectively to germination sensu stricto and post-germinative growth. Results are the mean ± SE of three replicates

slightly during early stages of germination and increasing slightly during post-germinative growth.

Ammonium assimilation pathway assessed by $^{15}NH_4$ labeling during post-germinative growth

The respective roles of GS and GDH in ammonium assimilation were investigated in vivo by $^{15}NH_4$ labeling during post-germinative growth. This period is characterized by an increase in ammonium release and amino acid neosynthesis and interconversion. Test and control seeds were germinated for 19 h on sterile water, and then transferred for 10 h to a labeling medium containing 2 mM $(^{15}NH_4)_2SO_4$ (99% atom excess). Test seeds were treated with the GS inhibitor MSX (5 mM) over the time course of the whole experiment.

MSX treatment resulted in a 94% inhibition of GS activity while GDH did not seem to be affected (data not shown). The most striking result of this experiment was that the assimilatory pathway of ammonium was completely inhibited in the seeds in which GS was inhibited by MSX. ^{15}N labeling in Glu, Asp, Gln and Asn was too low to be determined accurately in MSX-treated samples. In the controls, however, ammonium incorporation into organic forms was not inhibited. The results are expressed as a percentage of ^{15}N excess in each amino acid (Fig. 7). In the embryo axis, the most labeled amino acids were Gln [40.8% singly labeled (amido group) and 23.8% doubly labeled], Asn [17.34% singly labeled (amido group) and 8.6% doubly labeled] and Glu (5.6%). Significant label was also recovered in other amino acids, such as Ala (8.6%). In cotyledons, labeled nitrogen was recovered essentially in two amino acids singly (13.6%) and doubly (6.9%) labeled Gln, and singly labeled Asn (7.2%).

Discussion

Physiological and molecular characterization of N metabolism during germination and post-germinative growth in *Medicago truncatula*

Imbibition of *M. truncatula* seeds resulted in the activation of carbon and nitrogen metabolisms during the very early stages of germination, as revealed by changes in soluble sugars and amino acids contents. Comparison of the composition of the free amino acid pool with the composition of protein amino acids indicates that high amino acid inter-conversion take place in cotyledons after protein degradation and in the embryo axis after amino acid import. Because of the central role of Glu/Gln in amino acid inter-conversion during the germination process (Lea and Joy 1983; Limami et al. 2002), molecular characterization of the isoforms of the enzymes involved in the synthesis of these amino acids was undertaken. In *M. truncatula*, the genes for two cytosolic GS isoforms, GS1a and GS1b are expressed differentially in roots, leaves, stems and petioles (Stanford et al. 1993). The isoform GS1b appears to fulfill rather ubiquitous functions in ammonium assimilation and detoxification whereas GS1a, which is highly abundant in vascular tissue, seemed rather involved in the production of long-distance transport compounds of nitrogen (Carvalho et al. 2000). In germinating *M. truncatula* seeds, we found that *GS1b* expression was about 10-fold higher than that of *GS1a*. This finding suggests that GS1b is probably the isoform responsible for the reassimilation of ammonium released from protein and amino acids catabolism. Expression of *GS1a* was maintained at a low level, probably due to the small requirement for long-distance transport of nitrogen compounds at very early stages of germination. Our results agree with those of Carvalho et al. (2000) who showed that while chloroplast GS2 abundance decreased during senescence of *M. truncatula* leaves the expression of cytosolic *GS* increased, with *GS1b* being specifically localized in mesophyll cells and *GS1a* specifically localized in vascular elements. It is interesting to note that dedication of GS isoforms to specific metabolic roles was conserved even in different organs at different stages of development.

Two isoforms of GOGAT dependent on reduced ferredoxin or NADH are found in plants. In germinating *M. truncatula*, expression of the NADH-dependent

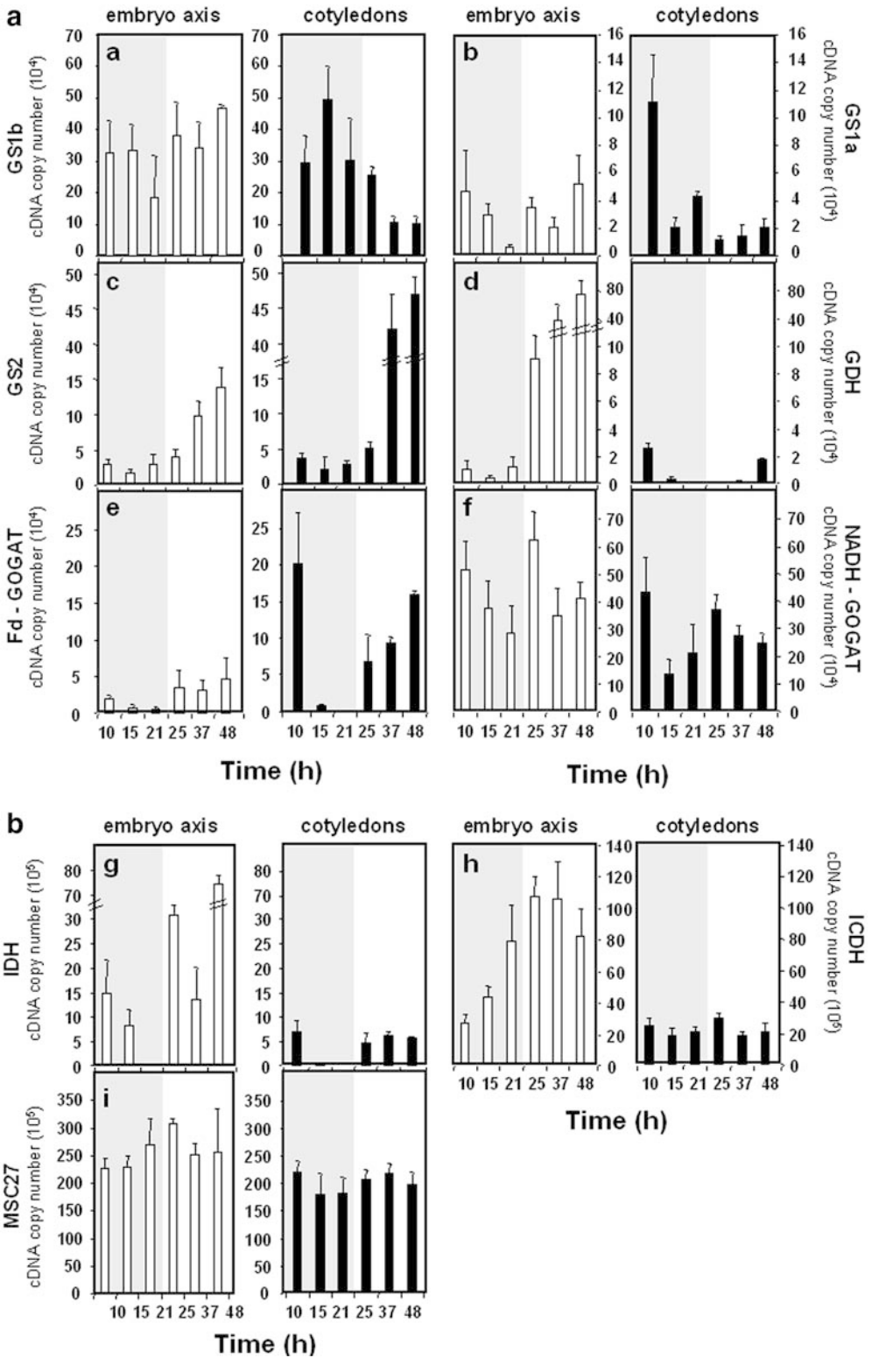

Fig. 4a–i Expression of genes encoding *GS1b* (**a**); *GS1a* (**b**); *GS2* (**c**); *GDH* (**d**); *Fd-GOGAT* (**e**); *NADH-GOGAT* (**f**); mitochondrial *IDH* (**g**); cytosolic *ICDH* (**h**) and *MSC27* (housekeeping gene; **i**) in cotyledons (*black columns*) and embryo axis (*white columns*) sampled at various times throughout germination and post-germinative growth of *M. truncatula*. Amplified fragments of each gene were cloned into pGEM-T Easy vector (Promega). The plasmids were diluted several times to generate templates ranging from 10^5 to 10^3 copies used for standard curves for estimation of copy numbers. *Shaded* and *non-shaded* areas correspond respectively to germination sensu stricto and post-germinative growth. The results are expressed as copy number of cDNA corresponding to each gene studied in 5 µl of first strands. Results are the mean ± SE of three replicates

isoform is predominant essentially in the embryo axis where it showed an important increase during post-germinative growth when the amino acids synthesis was at its utmost. This result substantiates the idea that NADH-GOGAT is rather associated with ammonium assimilation and/or remobilization of imported Gln in non-photosynthesizing organs such as nitrogen-fixing root nodules (Trepp et al. 1999a), roots and seeds (Hayakawa et al. 1999). Promoter studies have shown that *NADH-GOGAT* is expressed in vascular parenchyma

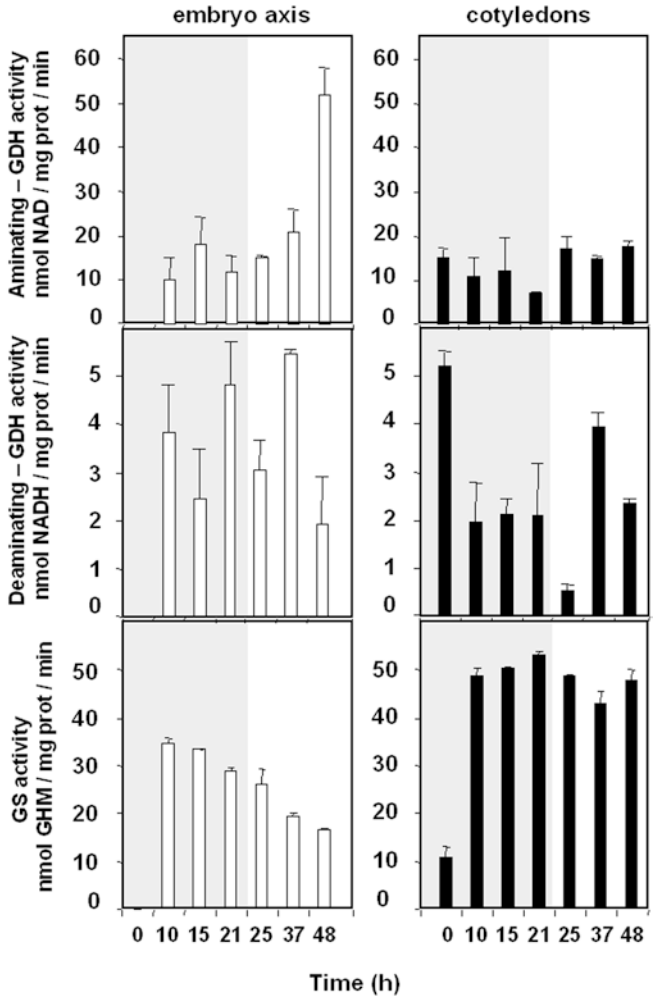

Fig. 5 Changes in in vitro activities of aminating and deaminating glutamate dehydrogenase (NADH-GDH and NAD-GDH) and glutamine synthetase (GS) in cotyledons (*black columns*) and embryo axis (*white columns*) throughout germination and post-germinative growth of *M. truncatula*. *Shaded* and *non-shaded* areas correspond respectively to germination sensu stricto and post-germinative growth. Results are the mean ± SE of three replicates

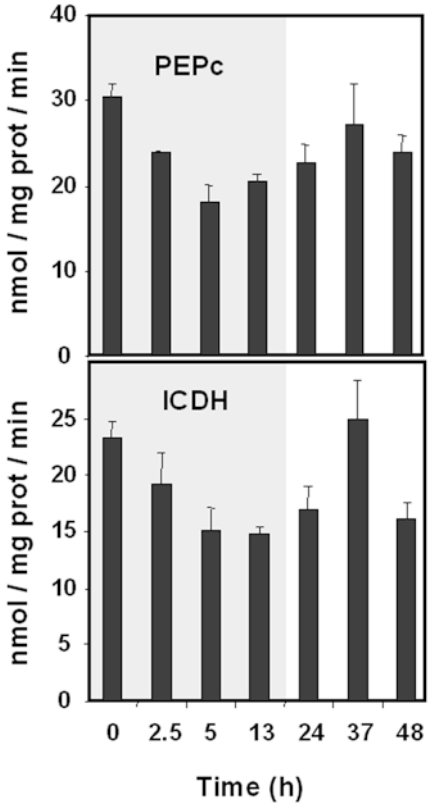

Fig. 6 Changes in activities of phosphoenopyruvate carboxylase (PEPc) and isocitrate dehydrogenase (I(C)DH) in seeds of *M. truncatula* throughout germination and post-germinative growth. *Shaded* and *non-shaded* areas correspond respectively to germination sensu stricto and post-germinative growth. Results are the mean ± SE of three replicates

cells and the nucellar epidermis of young grains of rice (Hayakawa et al. 1994).

Before radicle protrusion, the level of expression of the gene encoding the plastidic isoform *GS2* was very low in both embryo axis and cotyledons, indicating that this isoform does not contribute to ammonium assimilation during germination sensu stricto. However, despite the fact that seeds were maintained in darkness, *GS2* expression increased significantly in cotyledons but not in the embryo axis during post-germinative growth. Taken together, our results show that the cytosolic GS1b/NADH-GOGAT cycle constitutes the major route of assimilation of ammonium derived from reserve mobilization and Glu/Gln synthesis in heterotrophic seedlings of *M. truncatula* during germination sensu stricto and in the embryo axis during post-germinative growth maintained in darkness and in the absence of an exogenous source of nitrogen (NO_3^-). In cotyledons, however, during post-germinative growth the major route of ammonium assimilation is constituted by the couple GS2/Fd-GOGAT.

The cotyledon-enhanced expressions of *GS2* and *Fd-GOGAT* in the absence of light show that other signals related to developmental changes in cotyledons during the transition from germination to post-germinative growth trigger a shift of the main pathway of ammonium assimilation from the GS1b/NADH-GOGAT to the GS2/Fd-GOGAT cycle. These results are in agreement with the predominant role of GS2/Fd-GOGAT in ammonium assimilation in green mesophyll cells (Ziegler et al. 2003).

Relationship between carbon and nitrogen metabolism during germination and post-germinative growth in *M. truncatula*

At the onset of germination, the increase in sucrose in cotyledons revealed starch degradation while the accumulation of glucose and fructose in the embryo axis probably results from the import and further breakdown of sucrose in this organ. Two major connecting points

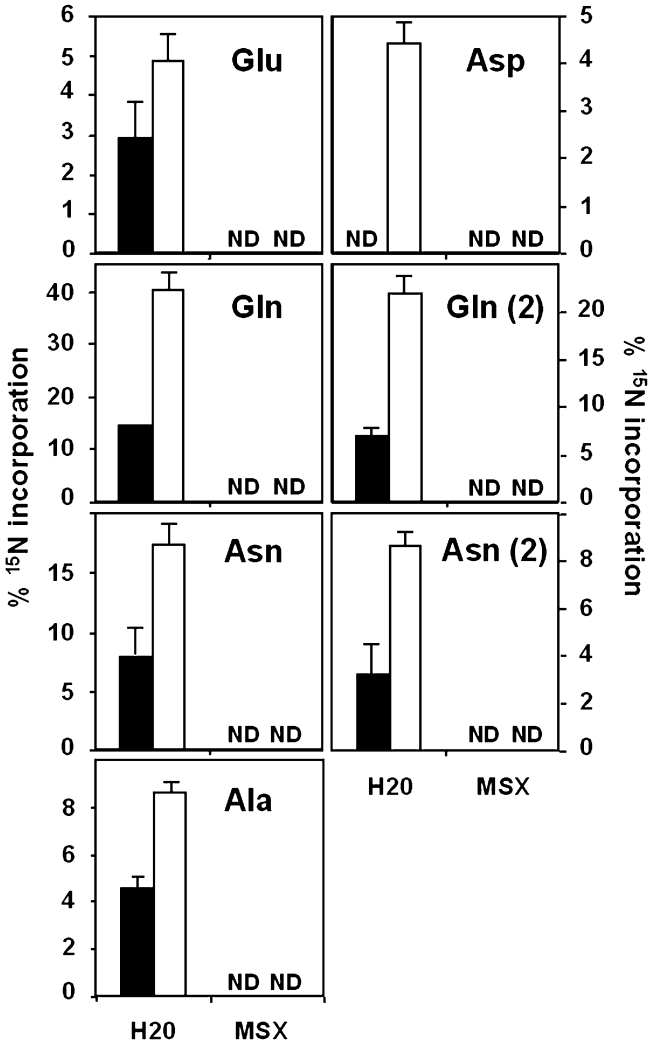

Fig. 7 $^{15}NH_4^+$ labeling experiment for determination of glutamate dehydrogenase (GDH) activity in vivo during post-germinative growth of *M. truncatula*. Seeds germinated for 19 h were fed with 2 mM $(^{15}NH_4)_2SO_4$ (99% ^{15}N atom excess) for 10 h in the presence or absence of 5 mM methionine sulfoximine (*MSX*), a GS inhibitor. Results are the mean ± SE of two replicates, corresponding to % ^{15}N in glutamate (*Glu*), aspartate (*Asp*), glutamine [*Gln*, singly and doubly *(2)* labeled], asparagine [*Asn*, singly and doubly *(2)* labeled] and alanine (*Ala*) in cotyledons (*black columns*) and embryo axis (*white columns*)

between carbon and nitrogen metabolisms are the reactions catalyzed by PEPc and I(C)DH, which generate carbon skeletons readily used for amino acid synthesis. Actually, these enzymes showed their highest activities in germinating *M. truncatula* seed during post-germinative growth when metabolic activity, in general, and amino acid synthesis, in particular, were increasing sharply. Accumulation of oxaloacetate in cotyledons but not in the embryo axis probably indicates the importance of the anaplerotic role of PEPc in the generation of asparagine, the amino acid transported in legumes. While the role of PEPc in germinating seeds has already been pointed out (Gonzalez et al. 1998; Limami et al. 2002), little is known about I(C)DH. Several isoforms of I(C)DH, with different cellular locations and electron donors, co-exist in plants. They have mainly been studied in vegetative tissues such as leaves and roots in relation to photorespiration-derived ammonium detoxification or primary nitrogen assimilation (Lancien et al. 2000). Expression of *ICDH* was 2–4 times higher than that of *IDH* in both embryo axis and cotyledons, providing an argument in favor of ICDH being the 2-oxoglutarate provider for amino acid synthesis. This result agrees with the idea that ICDH is rather involved in metabolic functions related to Glu/Gln production for import/export into different tissues (Lancien et al. 2000). In senescing potato leaves, both ICDH activity and transcript level increased (Fieuw et al. 1995), while transgenic potato expressing antisense *ICDH*, with only 8% of ICDH, did not show any noticeable alteration in C and N metabolism or amino acid synthesis (Kruse et al. 1998; Lancien et al. 2000). Furthermore, high expression of *ICDH* in germinating seed could be related to a specific role of this enzyme in developing tissue that is not related to the GS/GOGAT cycle (Palomo et al. 1998). In differentiating hypocotyls of Scots pine, ICDH has been associated with the supply of 2-oxoglutarate to dioxygenases. Dioxygenases are involved in different metabolic pathways including phytohormone synthesis, flavonoid and alkaloid biosynthesis, and hydroxylation of proline residues of extensins (hydroxyproline-rich glycoproteins; Palomo et al. 1998).

Besides the major connecting points between C and N metabolisms mentioned above, other links may be activated as a result of adaptation to specific physiological conditions. Consistent with this idea, accumulation of Ala in the embryo axis may result from the activation of this effective mechanism used in plants to conserve carbon skeletons that would be lost by ethanol glycolysis (Good and Muench 1992; Muench and Good 1994). The ^{15}N labeling experiment showed that besides Gln, Glu, Asn and Asp, Ala was the only other amino acid rapidly and significantly labeled. In fact, the morphological and biochemical characteristics of seeds lead to an oxygen deficiency in seed tissue during development and germination (Rolletschek et al. 2002). Elevated levels of Ala have been observed in oxygen-deficient roots; also, an alanine aminotransferase (AlaAT)-lacking glyoxylate aminotransferase activity is induced by hypoxia in barley (*Hordeum vulgare*), corn (*Zea mays*), and *Piptatherum miliaceum* roots (Good and Muench 1992; Muench and Good 1994). In rice (*Oryza sativa*), an AlaAT gene is expressed in the starchy endosperm tissue of maturing seeds where it is proposed to play a role in nitrogen transport during seed maturation (Kikuchi et al. 1999).

^{15}N-labeling evidence for GDH deaminating activity during post-germinative growth in *M. truncatula*

Among the studied enzymes, GDH showed the highest increase, up to 80-fold in gene expression, accompanied

by a consistent increase in the amount of GDH protein (data not shown) in the embryo axis during post-germinative growth. In the same period the amount of free ammonium increased sharply in the embryo axis (Fig. 1). The induction of *GDH* expression by ammonium has been shown in *Arabidopsis thaliana*, and it has been proposed that GDH has an accessory role, in addition to the GS/GOGAT cycle, in nitrogen assimilation under specific physiological conditions leading to high amounts of ammonium (Melo-Oliveira et al. 1996; Masclaux-Daubresse et al. 2002). A question is raised then about a possible involvement of GDH in assimilation of ammonium derived from the amino acid catabolism in the embryo axis. From our $^{15}NH_4$ labeling experiment, it appears that although in vitro aminating GDH activity was higher than deaminating activity, GDH does not contribute to ammonium assimilation either in the embryo axis or in cotyledons during post-germinative growth in *M. truncatula*. The discrepancy between the in vivo and in vitro results suggests that GDH is regulated in vivo by post-translational modifications allowing it to function in the catabolic direction. These modifications are not operational in vitro. What then would be the physiological contribution of GDH to N and C metabolisms in germinating seeds? An anapleurotic role as a 2-oxoglutarate provider has been proposed to explain the increase in GDH in senescing tobacco leaves, but this hypothesis suffers a lack of coherence since in terms of balance the carbon skeleton produced by Glu catabolism would be consumed by the assimilation of ammonium released during the same reaction (Masclaux-Daubresse et al. 2002). Furthermore, two enzymes that funnel carbon skeletons to nitrogen metabolism are active in the germinating seed, i.e. PEPc and I(C)DH. In our opinion, the physiological role of GDH in the embryo axis is linked to the central role of Glu in inter-conversion of imported amino acids. Catabolism of Glu by GDH seems to be one of the major sources of ammonium in seeds for Gln synthesis by GS in the absence of primary nitrogen (NO_3^-) assimilation. Furthermore, this reaction produces reducing power (NADH) in heterotrophic seedlings deprived of photosynthesis. However, besides its metabolic role, Glu is a precursor of proline (Brugière et al. 1999), γ-butyric acid and arginine, which is itself a precursor of polyamines and nitric oxide, the latter being a stress-related molecule in plants (Galili 2000). Glutamate has also been proposed to intervene as a signaling molecule that regulates plant growth and response to the environment. This idea is strongly supported by the fact that plants possess functional homologues of animal Glu receptors (Lam et al. 1998; Galili et al. 2001). Consistent with its stress-related and signaling role, Glu content might be highly regulated: in general, it is maintained at a constant level in plants. In the present work, in both embryo axis and cotyledons, Glu was maintained at a low and remarkably constant level, most probably due to a balance between synthesis and degradation. We suggest, then, that GDH catabolic activity might contribute to the control of Glu homeostasis. However, intriguing questions, particularly on post-translational regulation of GDH, still need to be addressed to allow us to understand why ammonium, which stimulates GDH expression (Melo-Oliveira et al. 1996), is not assimilated by this enzyme.

Acknowledgements The authors are grateful to Professor R. Adams for kindly correcting the English. We thank B. Jettner (Seed-Co Australia Co-Operative Ltd., Hilton, Australia) for the generous gift of *M. truncatula* cv. Paraggio seeds.

References

Aubert S, Bligny R, Douce R, Gout E, Ratcliffe RG, Roberts JKM (2001) Contribution of glutamate dehydrogenase to mitochondrial glutamate metabolism studied by ^{13}C and ^{31}P nuclear magnetic resonance. J Exp Bot 52:37–45

Baskin CC, Baskin JM (1998) Seeds: ecology, biogeography, and evolution of dormancy and germination. Academic Press, San Diego

Bergmeyer HU (1965) Citrate, malate, α-ketoglutarate. In: Bergmeyer HU (ed) Methods of enzymatic analysis. Academic Press, New York; Verlag Chemie, Weinheim, pp 318–334

Bewley JD (1997) Seed germination and dormancy. Plant Cell 9:1055–1066

Bradford MM (1976) A rapid and sensitive method for the quantitation of microgram quantities of protein utilizing the principle of protein–dye binding. Anal Biochem 72:248–254

Brugière N, Dubois F, Limami AM, Lelandais M, Roux Y, Sangwan RS, Hirel B (1999) Glutamine synthetase in the phloem plays a major role in controlling proline production. Plant Cell 11:1995–2011

Carvalho H, Lima L, Lescure N, Camut S, Salema R, Cullimore J (2000) Differential expression of the two cytosolic glutamine synthetase genes in various organs of *Medicago truncatula*. Plant Sci 159:301–312

Eastmond PJ, Graham IA (2001) Re-examining the role of the glyoxylate cycle in oilseeds. Trends Plant Sci 6:72–78

Eastmond PJ, Germain V, Lange PR, Bryce JH, Smith SM, Graham IA (2000) Postgerminative growth and lipid catabolism in oilseeds lacking the glyoxylate cycle. Proc Natl Acad Sci USA 97:5669–5674

Ferrario-Mery S, Hodges M, Hirel B, Foyer CH (2002) Photorespiration-dependent increase in phosphoenolpyruvate carboxylase, isocitrate dehydrogenase and glutamate dehydrogenase in transformed tobacco plants deficient in ferredoxin-dependent glutamine-α-ketoglutarate aminotransferase. Planta 214:877–886

Fieuw S, Müller-Röber B, Galvez S, Willmitzer L (1995) Cloning and expression analysis of the cytosolic $NADP^+$-dependent isocitrate dehydrogenase from potato. Plant Physiol 107:905–913

Finkelstein RR, Lynch TJ (2000) Abscisic acid inhibition of radicle emergence but not seedling growth is suppressed by sugars. Plant Physiol 122:1179–1186

Fricke W, Pahlich E (1992) Malate: a possible source of error in the NAD glutamate dehydrogenase assay. J Exp Bot 43:1515–1518

Galili G (2000) New insights and the regulation and functional significance of lysine metabolism in plants. Annu Rev Plant Biol 53:27–43

Galili G, Tang G, Zhu X, Gakiere B (2001) Lysine catabolism: a stress and development super-regulated metabolic pathway. Curr Opin Plant Biol 4:261–266

Gallardo K, Job C, Groot SPC, Puype M, Demol H, Vandekerckhove, Job D (2002) Proteomics of *Arabidopsis* seed germination. A comparative study of wild-type and gibberellin-deficient seeds. Plant Physiol 129:823–837

Garciarrubio A, Legaria JP, Covarrubias A (1997) Abscisic acid inhibits germination of mature *Arabidopsis* seeds by limiting the availability of energy and nutrients. Planta 203:182–187

Gonzalez MC, Osuna L, Echevarria C, Vidal J, Cejudo FJ (1998) Expression and localization of phospho *enol*pyruvate carboxylase in developing and germinating wheat grains. Plant Physiol 116:1249–1258

Good AG, Muench DG (1992) Purification and characterization of an anaerobically induced alanine aminotransferase from barley roots. Plant Physiol 99:1520–1525

Hayakawa T, Nakamura T, Hattori F, Mae T, Ojima K, Yamaya T (1994) Cellular localization of NADH-dependent glutamate-synthase protein in vascular bundles of unexpanded leaf blades and young grains of rice plants. Planta 193:455–460

Hayakawa T, Hopkins L, Peat LJ, Yamaha T, Tobin AK (1999) Quantitative intercellular localization of NADH-dependent glutamate synthase protein in different types of root cells in rice plants. Plant Physiol 119:409–416

Kikuchi H, Hirose S, Toki S, Akama K, Takaiwa F (1999) Molecular characterization of a gene for alanine aminotransferase from rice (*Oryza sativa*). Plant Mol Biol 39:149–59

Koorneef M, Bentsink L, Hilhorst H (2002) Seed dormancy and germination. Curr Opin Plant Biol 5:33–36

Kruse A, Fieuw S, Heineke D, Müller-Röber B (1998) Antisense inhibition of cytosolic NADP-dependent isocitrate dehydrogenase in transgenic tobacco plants. Planta 205:82–91

Lam HM, Chiu J, Hsieh MH, Meisel L, Oliveira IC, Shin M, Corruzi G (1998) Glutamate-receptor genes in plants. Nature 396:125–126

Lancien M, Gadal P, Hodges M (2000) Enzyme redundancy and the importance of 2-oxoglutarate in higher plant ammonium assimilation. Plant Physiol 123:817–824

Lea PJ, Joy KW (1983) Amino acid interconversion in germinating seeds. In: Nozzolillo C, Lea PJ, Loewus FA (eds) Mobilization of reserves in germination. Plenum, London, pp 77–109

Lea PJ, Miflin BJ (1974) An alternative route for nitrogen assimilation in higher plants. Nature 251:614–616

Limami AM, Rouillon C, Glevarec G, Gallais A, Hirel B (2002) Genetic and physiological analysis of germination efficiency in maize in relation to nitrogen metabolism reveals the importance of cytosolic glutamine synthetase. Plant Physiol 130:1860–1870

Masclaux-Daubresse C, Valadier MH, Carrayol E, Reisdorf-Cren M, Hirel B (2002) Diurnal changes in the expression of glutamate dehydrogenase and nitrate reductase are involved in the C/N balance of tobacco source leaves. Plant Cell Environ 25

Melo-Oliveira R, Oliveira IC, Coruzzi GM (1996) *Arabidopsis* mutant analysis and gene regulation define a nonredundant role for glutamate dehydrogenase in nitrogen assimilation. Proc Natl Acad Sci USA 93:4718–4723

Miflin BJ, Habash DZ (2002) The role of glutamine synthetase and glutamate dehydrogenase in nitrogen assimilation and possibilities for improvement in the nitrogen utilization of crops. J Exp Bot 53:979–987

Miflin BJ, Lea PJ (1980) Ammonia assimilation. In: Miflin BJ, Con EE (eds) The biochemistry of plants, vol 5. Academic Press, New York pp 169–202

Morot-Gaudry J-F, Job D, Lea PJ (2001) Amino acid metabolism. In: Lea PJ, Morot-Gaudry JF (eds) Plant nitrogen. Springer, Berlin Heidelberg New York, pp 167–211

Muench DG, Good AG (1994) Hypoxically inducible barley alanine aminotransferase: cDNA cloning and expression analysis. Plant Mol Biol 24:417–27

Palomo J, Gallardo F, Suarez MF, Canovas FM (1998) Purification and characterization of NADP-linked isocitrate dehydrogenase from Scots pine. Evidence for different physiological roles of the enzyme in primary development. Plant Physiol 118:617–626

Pritchard SL, Charlton WL, Baker A, Graham IA (2002) Germination and storage reserve mobilization are regulated independently in *Arabidopsis*. Plant J 31:639–647

Rhodes D, Rich PJ, Brunk DG (1989) Amino acid metabolism of *Lemna minor* L. Plant Physiol 89:1161–1171

Robinson SA, Slade AP, Fox GG, Phillips R, Ratcliffe G, Stewart GR (1991) The role of glutamate dehydrogenase in plant nitrogen metabolism. Plant Physiol 95:509–516

Robinson SA, Stewart GR, Phillips R (1992) Regulation of glutamate dehydrogenase activity in relation to carbon limitation and protein catabolism in carrot cell suspension cultures. Plant Physiol 98:1190–1195

Rolletschek H, Borisjuk L, Koschorreck M, Wobus U, Weber H (2002) Legume embryos develop in a hypoxic environment. J Exp Bot 53:1099–1107

Stanford AC, Larsen K, Barker DG, Cullimore JV (1993) Differential expression within the glutamine synthetase gene family of the model legume *Medicago truncatula*. Plant Physiol 103:73–81

Stewart GR, Shatilov VR, Turnbull MH, Robinson SA, Goodall R (1995) Evidence that glutamate dehydrogenase plays a role in the oxidative deamination of glutamate in seedlings of *Zea mays*. Aus J Plant Physiol 22:805–809

Swarup R, Bennett MJ, Cullimore JV (1990) Expression of glutamine synthetase genes in cotyledons of germinating *Phaseolus vulgaris* L. Planta 183:51–56

Trepp GB, Van de Mortel M, Yoshioka H, Miller S, Samac DA, Gantt JS, Vance CP (1999a) NADH-Glutamate synthase in alfalfa root nodules. Genetic regulation and cellular expression. Plant Physiol 119:817–828

Trepp GB, Plank DW, Gantt JS, Vance CP (1999b) NADH-Glutamate synthase in alfalfa root nodules. Immunocytochemical localization. Plant Physiol 119:829–837

Vincent R, Fraisier V, Chaillou S, Limami MA, Deleens E, Phillipson B, Douat C, Boutin JP, Hirel B (1997) Overexpression of a soybean gene encoding cytosolic glutamine synthetase in shoots of transgenic *Lotus corniculatus* L. plants triggers changes in ammonium assimilation and plant development. Planta 201:424–433

Watanabe A, Hamada K, Yokoi A, Watanabe A (1994) Biphasic and differential expression of cytosolic glutamine synthetase genes of radish during seed germination and senescence of cotyledons. Plant Mol Biol 26:1807–1817

Yamaya T, Oaks A, Rhodes D, Matsumoto H (1986) Synthesis of [^{15}N]glutamate from [^{15}N]H_4^+ and [^{15}N]glycine by mitochondria isolated from pea and corn roots. Plant Physiol 81:754–757

Ziegler C, Feraud M, Jouglet T, Viret L, Spampinato A, Paganelli V, Ben Hammouda M, Suzuki A (2003) Regulation of promoter activity of ferredoxin-dependent glutamate synthase. Plant Physiol Biochem 41:649–655